Journal of Materials and Environmental Sciences
ISSN : 2028-2508

JMES, 2017 Volume 8, Issue 2, Page 573-581

http://www.jmaterenvironsci.com/

CO_2 reforming of CH_4 over Ni/SBA-15: Influence of Ni loading on the metal-support interaction and catalytic activity

H.D. Setiabudi[a,*], K.H. Lim[a], N. Ainirazali[a], S.Y. Chin[a], N.H.N. Kamarudin[b]

[a]*Faculty of Chemical and Natural Resources Engineering, Universiti Malaysia Pahang, 26300 Gambang, Kuantan, Pahang, Malaysia.*

[b]*Department of Chemical and Process Engineering, Faculty of Engineering and Built Environment, Universiti Kebangsaan Malaysia, 43600 UKM Bangi, Selangor, Malaysia.*

Received 05 Jul 2016,
Revised 22 Nov 2016,
Accepted 25 Nov 2016

Keywords

- ✓ Ni/SBA-15,
- ✓ CH_4 reforming,
- ✓ Nickel loading,
- ✓ metal-support interaction,
- ✓ catalyst stability

Email:herma@ump.edu.my (H.D. Setiabudi);
Phone: +60-9-5492836;
Fax: +60-9-5492889

Abstract

The influence of Ni loading on the properties of Ni/SBA-15 and CO_2 reforming of CH_4 were studied. XRD, BET and TGA results indicated that the increasing Ni loading (3–10 wt%) decreased the crystallinity, surface area and physically adsorbed water content of the catalysts. FTIR, TEM and H_2-TPR analysis confirmed the formation of Ni–O–Si by the substitution of surface silanol groups with Ni species and the maximum substitution of surface silanol groups with Ni were achieved at 5 wt%, while further increased in Ni loading stimulate the agglomeration of Ni particles. The activity of catalysts followed the order of 5Ni/SBA-15 > 3Ni/SBA-15 ≈ 10Ni/SBA-15 > SBA-15, with the conversion of CH_4 and CO_2 over 5Ni/SBA-15 was about 89% and 88% respectively, and CO_2/CH_4 ratio of 1.02. The superior catalytic performance of 5Ni/SBA-15 towards CO_2 reforming of CH_4 probably was related with the formation of metal-support interaction, Ni–O–Si, which enhanced the stabilization of the active Ni species on SBA-15 support and altered the properties of catalyst towards an excellent catalytic performance. The analysis of spent catalysts found that the presence of Ni–O–Si minimizes the growth of encapsulating graphite carbon and thus enhanced the stability of catalyst. This study provides new perspectives on the Ni-based catalyst, particularly on the influence of Ni on the metal-support interaction and catalytic performance of Ni/SBA-15 towards CO_2 reforming of CH_4.

1. Introduction

In recent years, climax change has become a serious world-wide environmental problem and the negative effects of greenhouse gas emission on people's health are unavoidable fact. As CO_2 is one of the main contributors to the greenhouse effect and hence causes climate change, the elimination of CO_2 has been an attracting interest from the environmental perspective. The CO_2 reforming of CH_4 (so-called dry reforming) is one of the CO_2 elimination methods and has recently attracted considerable attention [1-3], due to the simultaneous utilization and reduction of two greenhouse gases, CO_2 and CH_4, into synthesis gas (syngas). The syngas produced has a lower H_2/CO ratio than those available in industrial processes, which is preferred for the synthesis of valuable oxygenated chemicals and long-chain hydrocarbons.

The CO_2 reforming of CH_4 has been studied extensively using variety of supported metal catalysts including transition metal-based catalysts (Ni, Co, Cu, Fe) [4-8] and noble metal-based catalysts (Rh, Ru, Pd, Pt, Ir) [9-11]. It has been reported that noble metal-based catalysts especially Rh based ones have the higher stability and resistance against coke deposition [12]. However, restricted availability and high cost limited their use in industrial level. Therefore, the substitution of noble metals by transition ones, especially Ni [2,13] is nowadays attractive owing to its wider availability, lower cost and better catalytic performance [14-15]

The catalytic activity of a catalyst is influenced by several factors such as the nature of the support [16-17], metal precursor [18] and the amount of metal loading [3,19-20]. It has been reported by several researchers that the amount of metal loading significantly influences the properties and activities of the catalysts towards CO_2 reforming of CH_4 [19,21]. In brief, the amount of metal content on the support affected the interaction of metal with the support, which further affecting the catalytic behaviour during the reaction. The metal species tend to be highly dispersed on the support material at low metal loading, whereas at high metal loading, the metal particles tend to aggregate and forming large particles. Thus, it is very important to determine the optimum metal loading of the catalyst for the specific reaction and understanding the relationship between the amount of metal loading with the properties and catalytic activities of the catalyst.

In particular, Ni-based mesoporous silica (SBA-15) was found to be active and stable for CO_2 reforming of methane [16,22] owing to the properties of SBA-15 that possesses high surface area (600-1000 m^2/g), thermal stability, a hexagonal structure of mesopores with size of 4.6-30 nm and thicker walls (3.1-6.4 nm) [23-24]. With regards to the importance of the amount of Ni loading on the catalytic performance of Ni/SBA-15, several research groups have studied the influenced of Ni loading on the several aspects of the study, including structural properties of catalysts [25], catalytic stability [26] and Ni sintering [16]. Although several studies have reported the effect of Ni loading on the catalytic performance of Ni/SBA-15, however, only a few publications concerning the influence of Ni loading on the metal-support interaction and its role towards an excellent catalytic performance are found. In addition, to the best of our knowledge, the detailed study of the Ni-O-Si interaction and its relationship on CO_2 reforming of CH_4 over Ni/SBA-15 has not yet been clearly reported. Therefore, this study reports the influence of Ni loading on the metal-support interaction and catalytic activity of Ni/SBA-15 towards CO_2 reforming of CH_4.

2. **Experimental**

2.1.*Catalysts Preparation*

The SBA-15 was prepared according to the method reported by Zhao et al. [23]. The triblock copolymer P123 ($EO_{20}PO_{70}EO_{20}$, Aldrich) was used as the structure-directing agent and tetraethyl orthosilicate (TEOS, Merck) as the silica source. The P123 was dissolved in the solution of deionized water and 2M hydrochloric acid solution and stirred at 40 ^oC for 1 h. The TEOS was slowly added to the mixture with vigorous stirring at 40 ^oC for 24 h, and the precipitate product was obtained. The precipitate product was filtered, washed with deionized water and dried overnight at 110 ^oC. The sample was calcined at 550 ^oC for 3 h to remove the triblock copolymer.

The Ni/SBA-15 catalyst was prepared by impregnation of SBA-15 powder with an aqueous solution of Ni salt precursor, $Ni(NO_3)_2{\cdot}6H_2O$ (Merck, 99%). The resulting slurry was heated slowly at 80 ^oC under continuous stirring and maintained at that temperature until nearly all the water had evaporated. The solid residue was dried overnight at 110 ^oC followed by calcination at 550 ^oC for 3 h. A series of samples with different Ni loading (3, 5 and 10 wt%) were prepared.

2.2 *Catalyst Characterization*

The crystalline structure of the catalyst was determined by X-ray diffraction (XRD) recorded on powder diffractometer (Philips X' Pert MPD, 3 kW) using a Cu-*Kα* radiation (λ = 1.5405Å). The primary crystallite size of NiO (D_{NiO}) was calculated by means of the Scherrer equation [27]:

$$D_{NiO} = \frac{0.9\lambda}{B\cos\theta} \quad (1)$$

Where λ is the X-ray wavelength corresponding to Cu-*Kα* radiation (0.15405 nm), *B* is the broadening (in radians) of the nickel (200) reflection and θ is the angle of diffraction corresponding to peak broadening. The Bruneuer-Emmett-Teller (BET) analysis of the catalyst was conducted using AUTOSORB-1 model AS1 MP-LP instrument at 77 K. Transmission electron microscopy (TEM) was carried out using a Philips CM12. The sample was dispersed in acetone by sonication, and deposited on an amorphous, porous carbon grid. The Fourier Transform Infrared (FTIR) analysis was carried out using Thermo Nicolet Avatar 370 DTGS model in KBr matrix in order to study the chemical properties of catalysts and to identify the interaction of Ni species with SBA-15. The phenomenon of weight loss, which results from heating the samples were analyzed by Thermogravimetric analysis (TGA) (TGA Q500,TA Instruments) under a mixture of air (20% O_2/80% N_2) with heating rate of 5 $^oC\ min^{-1}$ up to 900 °C. H_2-TPR analysis was carried out using Micromeritics Chemisob 2920 Pulse Chemisorption in 10% H_2/Ar at 10 $^oC\ min^{-1}$. Prior to the chemisorption, 30 mg of the catalyst was reduced with pure H_2 (20 mL min^{-1}) at 850 ^oC for 1 h. The amount of hydrogen uptake was determined by injecting mixed gas (10% H_2/Ar) periodically into the reduced catalyst.

2.3 *Catalytic Testing*

The catalytic CO_2 reforming of CH_4 was carried out in a microcatalytic reactor at atmospheric pressure and reaction temperature of 800 ^oC. Prior to the reaction, 0.2 g of catalyst was reduced in a H_2 flow of 50 ml/min for 3 h at 700 ^oC. The feeding gas flow rate to the reactor was set at 50 ml/min, with a ratio of CH_4:CO_2:N_2 = 1:1:1, and N_2 was used as a carrier gas. The effluent gas was analyzed with an Agilent gas chromatography equipped with a thermal conductivity detector (TCD). The CH_4 and CO_2 conversion were calculated according to the following equations;

$$CO_2 \quad Conversion, \quad X_{CO_2} = \frac{F_{CO_{2;in}} - F_{CO_{2;out}}}{F_{CO_{2;in}}} x100\% \tag{2}$$

$$CH_4 \quad Conversion, \quad X_{CH_4} = \frac{F_{CH_{4;in}} - F_{CH_{4;out}}}{F_{CH_{4;in}}} x100\% \tag{3}$$

Where F is the molar flow rate for particular compound. The product distribution ratio, H_2/CO was calculated based on equation (4).

$$\frac{H_2}{CO} = \frac{F_{H_2}}{F_{CO}} \tag{4}$$

3. **Results and discussion**

3.1. *Characterization of the catalysts*

Figure 1A shows the low-angle XRD patterns of SBA-15 and Ni/SBA-15 catalysts. The patterns exhibited three peaks, indexed as (100), (110) and (200) which are reflections of typical two dimensional, hexagonally ordered mesostructures (*p*6mm), demonstrating the high quality of the mesopore packing [23]. An increase of the Ni content from 3 to 10 wt% resulted in a slight decrease of the peaks, indicating structural degradation of SBA-15. The changes in the XRD peaks are more clearly seen by calculating the percentage crystallinity of the catalysts as shown in Table 1. The percentage crystallinity of SBA-15 was decreased from 100% to 85.4% with the introduction of Ni species (3 – 10 wt%), indicating the partial collapse of structure with the presence of Ni. The presences of Ni crystallites on the surface of catalysts were characterized using wide-angle XRD, as shown in Figure 1B. The peaks assigned to face-centered cubic crystalline NiO at 37.3°, 43.2°, 62.9°, 75.4° and 79.3° [28] were more intense with increasing Ni loading, in agreement with more crystalline phase of NiO on the SBA-15.

The textural properties of all catalysts are summarized in Table 1. For bare SBA-15, the BET surface area was 856 m^2/g with pore volume of 0.999 cm^3/g. However, the introduction of Ni from 3 to 10 wt% decreased the surface area and pore volume of SBA-15, indicating the blockage of the pores by Ni species. It is noted that the particles size of Ni species significantly increased with 10 wt% of Ni content might due to the agglomeration of Ni particles at higher amount of metal loading. Moreover, 10Ni/SBA-15 has slightly higher pore volume than 5Ni/SBA-15 which indicative of metal particle agglomeration leading to a slight contraction of the walls and consequently expansion of the pores. The change in the BET surface area of the catalyst caused by the different amounts of metal loading was also observed for Ni/MSN and Co/SBA-15 catalysts, reported by Aziz et al. [28] and Martínez [19], respectively. They found that increasing the amount of metal loading resulted to a decrease in the surface area of the support catalyst due to the blockage of the pores with metal species. Moreover, the presence of larger metal particles at higher amount of metal loading due to the agglomeration of metal particles was also reported for the same catalysts.

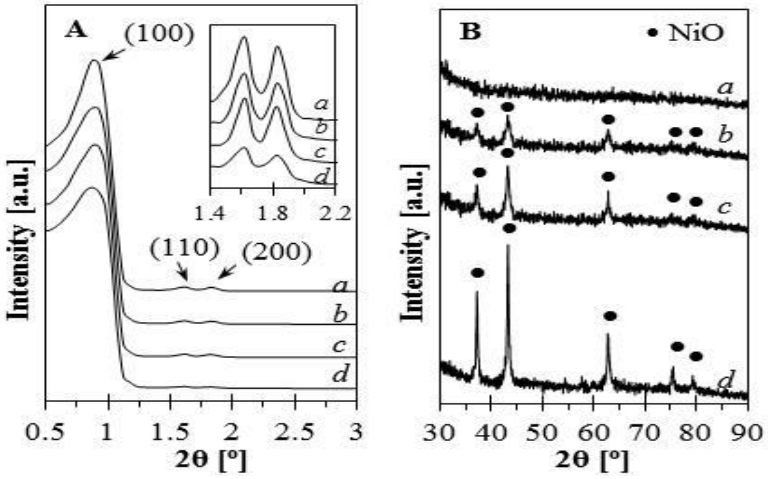

Figure 1: (A) Low and (B) wide angle XRD patterns of (a) SBA-15, (b) 3Ni/SBA-15, (c) 5Ni/SBA-15 and (d) 10Ni/SBA-15.

Table 1: Physical properties of SBA-15, 3Ni/SBA-15, 5Ni/SBA-15 and 10Ni/SBA-15.

Catalyst	Nickel content (wt%)	XRD crystallinity (%)	BET Surface Area (m^2/g)	Pore volume (cm^3/g)	Ni particle size (nm)[a]
SBA-15	0	100	856	0.999	-
3Ni/SBA-15	3	93.2	650	0.728	10.7
5Ni/SBA-15	5	91.3	473	0.649	13.6
10Ni/SBA-15	10	85.4	329	0.699	25.9

[a] Determine by XRD (Scherer equation)

The agglomeration of Ni particles at higher metal loading was investigated using TEM, as shown in Figure 2, in which the presence of Ni particles was observed by the occurrence of small spots with darker contrast areas. The 5Ni/SBA-15 catalyst showed the deposition of small Ni particles, whereas 10Ni/SBA-15 was contain of large-sized Ni particles due to the agglomeration of Ni particles at higher amount of Ni loading. In accordance with the XRD and BET results, it is believed that the higher amount of Ni loading will lead to agglomeration of Ni particles and thus increase the size of Ni particles.

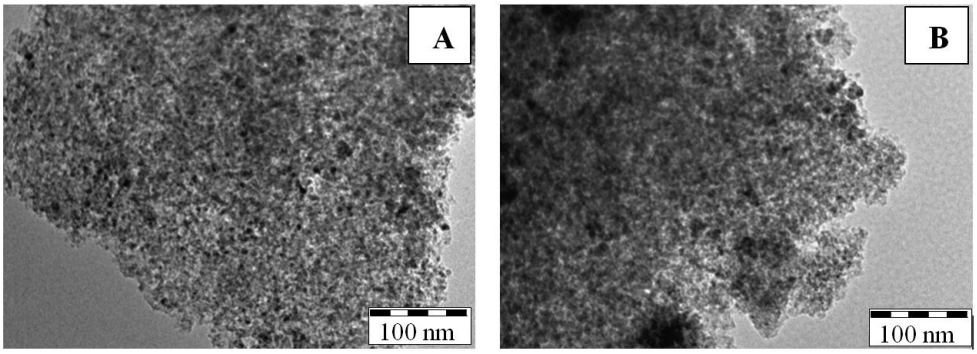

Figure 2: TEM images of (A) 5Ni/SBA-15 and (B) 10Ni/SBA-15.

Figure 3 shows the FTIR spectra of KBr in the range of 1400 – 500 cm^{-1} and 3800 – 2500 cm^{-1}. The bands in the range of 1400 and 500 cm^{-1} are attributed to the vibrations of the stretching and bending modes of Si-O units, while the bands in the range of 3800 and 2500 cm^{-1} are associated with O-H stretching vibration mode of Si-OH involved in hydrogen interaction with the adsorbed water molecules. The bands at approximately 1060 and 801 cm^{-1} corresponded to the asymmetric and symmetric stretching vibrations of Si–O–Si in the framework, respectively [29]. Meanwhile, the band at approximately 961 and 510 cm^{-1} corresponded to the Si–O stretching vibration of Si–OH groups and tetrahedral bending vibration of Si–O–Si bonds, respectively [30].

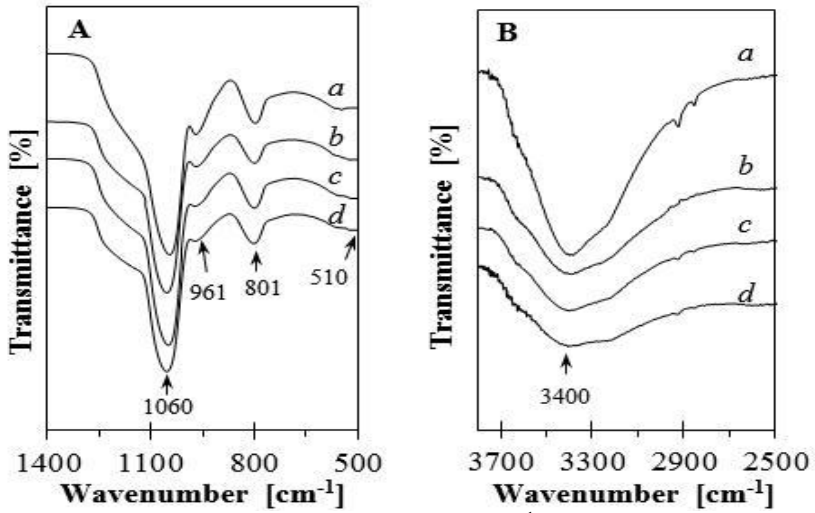

Figure 3: FTIR spectra of KBr in the range of (A) 1400 – 500 cm^{-1} and (B) 3800 – 2500 cm^{-1} of (a) SBA-15, (b) 3Ni/SBA-15, (c) 5Ni/SBA-15 and (d) 10Ni/SBA-15.

The introduction of Ni on SBA-15 did not alter the intensities of the bands at 1060, 801 and 510 cm^{-1} indicating neither asymmetric stretching, symmetric stretching nor tetrahedral bending of Si-O-Si interacted with Ni. However, the intensity of the band at 961 cm^{-1} decreased slightly and becomes enveloped in the peak of 1060 cm^{-1} indicating the formation of Ni–O bonds replacing the hydrogen atoms of Si–OH. Moreover, it was observed that an increase in Ni loading decreased the intensity of O–H stretching vibration mode of Si–OH involved in hydrogen interaction with the adsorbed water molecules at 3400 cm^{-1}, indicating the substitution of O–H with O–Ni. Therefore, the changes in the intensities of the bands at 3400 and 961 cm^{-1} are considered as a direct evidence for the formation of Si–O–Ni by substitution of O–H with O–Ni. The change of the SBA-15 structure caused by the introduction of metal was also observed on the Cu-SBA-15 catalyst reported by Brodie-Linder et al. [30]. They found that the intensity of the band assigned to Si–O stretching vibration of the Si–OH groups at 960 cm^{-1}disappears and becomes enveloped in the large Si–O framework peak at 1068 cm^{-1}owing to the formation of Cu–O bonds.

Figure 4 shows the TGA curves of SBA-15 and Ni/SBA-15 catalysts. The TGA results explained the phenomenon of weight loss, which results from heating the samples in a mixture of N_2 and O_2 flow. The curves of all catalyst showed a weight loss region in the range of 27 to 200 ^oC, indicating the loss of catalyst water content. The weight loss percentage was less significant with the introduction of Ni, indicating the reduction of catalyst water content in the presence of Ni. This result was related with the substitution of surface silanol groups with Ni species, which indirectly eliminated the hydrogen interaction between silanols and adsorbed water molecules. The weight loss percentage was decreased with an increase in Ni loading (3 – 5 wt%), and no further decreased was observed with increasing amount of Ni loading (up to 10 wt%). This result indicated that the maximum substitution of surface silanol groups with Ni species was achieved at 5 wt%, and further increase in Ni loading stimulate the agglomeration of Ni particles. Moreover, it was observed that none of the catalyst experienced the formation of intermediate compound upon increasing the temperature, indicating that all catalyst were thermally stable at high temperatures. The change of the weight loss percentage caused by the introduction of metal was also observed on the Ir-HZSM-5 [31] in which the weight loss of water was less pronounced when the HZSM-5 contains Ir.

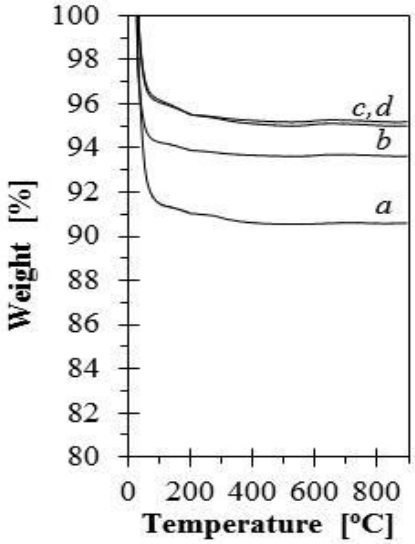

Figure 4: TGA curves of (a) SBA-15, (b) 3Ni/SBA-15, (c) 5Ni/SBA-15 and (d) 10Ni/SBA-15.

Figure 5 shows the TPR profile of the Ni/SBA-15 catalysts with various Ni loadings. In the case of 3Ni/SBA-15 and 5Ni/SBA-15, the deconvoluted TPR profile consists of four peaks centered at 380, 438, 490 and 540 ^oC. Meanwhile, the deconvoluted TPR profile of 10Ni/SBA-15 consists of four peaks centered at 380, 418, 460 and 520 ^oC. The decrease in the temperature of TPR peaks at 10Ni/SBA-15 might be due to the presence of agglomerate NiO particles which can easily migrate and aggregate during the reduction process. According to the Sidik et al. [2], the peaks in the low temperature zone (< 400 ^oC) are assigned to the reduction of Ni_2O_3 or NiO species, while the peaks in temperature higher than 400 ^oC are assigned to the reduction of NiO species which interacted with the support. In brief, the peaks in the medium temperature zone (400 to 500 ^oC) are assigned to the reduction of NiO species which have weak interaction with the support, while the peaks in the high temperature zone (500 to 600 ^oC) are assigned to the reduction of NiO species having medium strength interaction with the support [32].

The TPR data are categorized based on the temperature zone and the data are presented in Table 2. Based on the summarized information in Table 2, it was observed that an increase in Ni loading (up to 5 wt%) substantially increase the peak area of medium and high temperature zone, indicating the positive role of Ni in promoting the metal-support interaction. However, a further increase in the Ni loading from 5 to 10 wt% resulted in a significant increase in the peak area of low and medium temperature zone without changing the peak area of high temperature zone, indicating a dramatic increase in the amount of un-bound and weakly bound NiO species with the same amount of medium strength of NiO interaction. This result shows that the formation of medium strength of NiO interaction (Ni-O-Si) through the substitution of surface silanol groups with Ni species was achieved the maximum at 5 wt% and further increase in Ni loading stimulate the agglomeration of Ni particles which can easily migrate and aggregate during the reduction process.

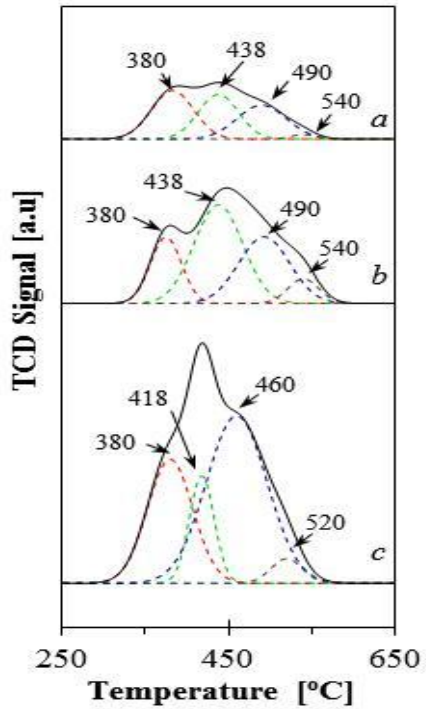

Figure 5: H_2-TPR profiles of (a) 3Ni/SBA-15, (b) 5Ni/SBA-15 and (c) 10Ni/SBA-15. The dotted line represents the Gaussian peaks.

Table 2: Deconvoluted H_2-TPR analysis of 3Ni/SBA-15, 5Ni/SBA-15 and 10Ni/SBA-15.

Catalyst	Peak Area		
	< 400 °C (low)	400 – 500 °C (medium)	500 – 600 °C (high)
3Ni/SBA-15	0.4643	0.7867	0.0268
5Ni/SBA-15	0.4646	1.8514	0.1736
10Ni/SBA-15	1.2618	2.8993	0.1736

3.2. *Catalytic testing*

Figure 6A and Figure 6B shows the effect of Ni loading on the conversion of CH_4 and CO_2 in CO_2 reforming of CH_4 at 800 °C. The reaction of bare SBA-15 showed lower activity (< 5% of CO_2 and CH_4 conversion), indicating that the metallic sites are necessary in the studied catalytic reaction. At temperature studied, 5Ni/SBA-15 exhibited an excellent performance with the highest stability as compared to 3Ni/SBA-15 and 10Ni/SBA-15. The effect of Ni loading on the performance of Ni/SBA-15 towards CO_2 reforming of CH_4 is more clearly illustrated in Figure 6C, in which the average of CH_4 conversion, CO_2 conversion and H_2/CO ratio were plotted as a function of Ni loading. The catalytic activity of Ni/SBA-15 towards CO_2 reforming of CH_4 followed the order of 5Ni/SBA-15 > 3Ni/SBA-15 ≈ 10Ni/SBA-15, whereas the average H_2/CO ratio followed the order of 5Ni/SBA-15 > 3Ni/SBA-15 > 10Ni/SBA-15. The 5Ni/SBA-15 catalyst exhibited an excellent performance with the conversion of CH_4 and CO_2 was about 89% and 88%, respectively and H_2/CO ratio of 1.02. The superior catalytic behavior of 5Ni/SBA-15 towards CO_2 reforming of CH_4 probably was related to the substitution of surface silanol groups with Ni species, which altered the properties of catalyst towards an

excellent catalytic performance. Meanwhile, a decreased in the catalytic performance with further increase in Ni loading (10 wt%) might be related to the agglomeration of Ni particles on the surface of SBA-15. The change in the activity of catalyst with metal loading was also observed on the $Ni/CeO_2/MgO$ catalyst, as reported by Khajenoori et al. [13]. They found that the increasing in Ni loading up to 10 wt% increased the conversion of CH_4 and CO_2, while, further increasing in Ni content more than 10 wt% decreased the activity of catalyst due to an increase in the Ni crystallite size at higher Ni loading. In addition, Sidik et al. [2] found that the higher catalytic properties of Ni/MSN is attributed to the strongest Ni-support interaction, while the lower catalytic activity of Ni/MSN is attributed to the inferior dispersion of Ni species as well as the larger Ni particles size arose from the weaker Ni-support interaction. Moreover, Rahemi et al. [33] also found that the dispersion and crystallite size of metal are vital factors in enhancing the catalytic activity of the catalyst. Based on this information, it can be assumed that the excellent catalytic activity of 5Ni/SBA-15 is closely related with the better dispersion of Ni particles on the surface of catalyst owing to the existence of the metal-support interaction (Si–O–Ni).

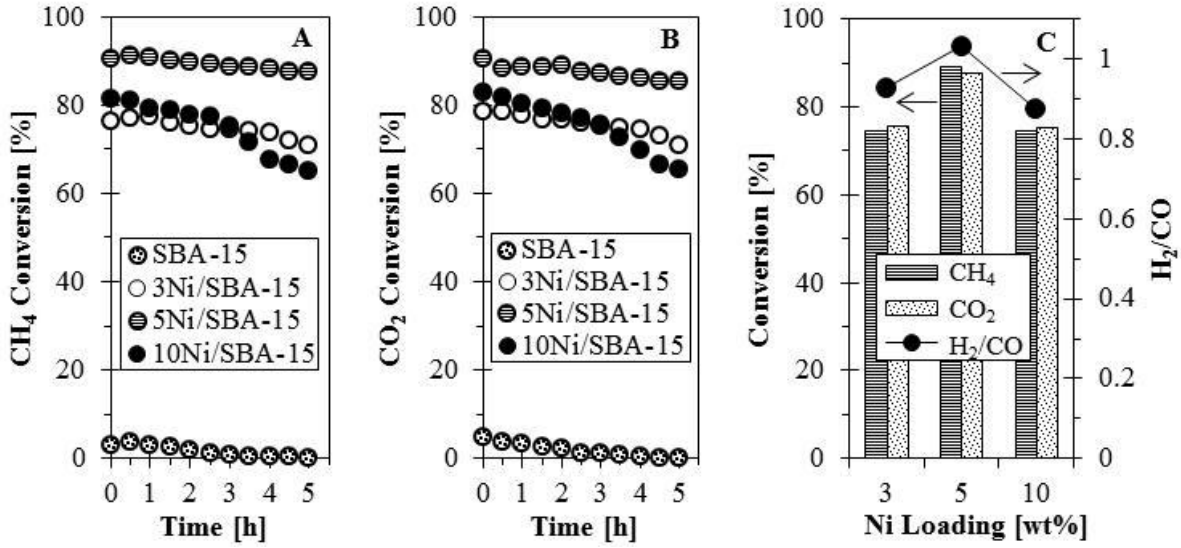

Figure 6: (A) CH_4 conversion and (B) CO_2 conversion of SBA-15, 3Ni/SBA-15, 5Ni/SBA-15 and 10Ni/SBA-15 in CO_2 reforming of CH_4. (C) Effect of Ni loading on the CH_4 conversion, CO_2 conversion and H_2/CO ratio.

According to the proposed mechanism for CO_2 reforming of CH_4, the stepwise adsorption of CH_4 followed by its decomposition into CH_x fragments occurs on active metal sites, whereas CO_2 activation occurs mainly over the supports [34]. Based on this information, it can be assumed that the excellent activity of 5Ni/SBA-15 is closely associated with the substitution of surface silanol groups with Ni species, which enhanced the stabilization of the active Ni species on SBA-15 support and altered the properties of catalyst towards an excellent catalytic performance. The relation of metal-support interactions with CO_2 reforming of CH_4 was also observed in TiO_x/Pt catalysts reported by Bradford and Vannice [35]. They found that the active sites for the CO_2 reforming of CH_4 are created in the metal-support interfacial region which promotes CH_4 dissociation and CO_2 dissociation. In addition, Sidik et al. [2] found that the higher catalytic activity of Ni/MSN towards CO_2 reforming of CH_4 was associated with the availability of a great number of active sites arose from the strong interaction between the Ni and the support. By referring to the previous studies, it is reasonable to conclude that the metal-support interaction (Si–O–Ni) are responsible for the formation of active sites, and thus resulted in higher catalytic performance.

3.3. *Characterization of the spent catalysts*

A quantitative analysis of carbon formation over the spent Ni/SBA-15 after 5 h reaction was investigated by TGA analysis and the results are shown in Figure 7. For all catalysts, the weight loss of the carbon residuals followed a two-stage pattern, a first one that slowly develops a broad reduction at 300 to 500 ^oC, and another one at temperature higher than 500 ^oC. According to the previous report [36], the oxidation of amorphous species occurs at low temperature (400 – 500 ^oC), while graphite carbon is oxidized at higher temperature (above 500 ^oC). Thus, the amount of carbon deposited on the surface of catalysts was quantified based on the percentage weight loss from 400 ^oC and above. Based on the calculation, the amount of carbon content followed

the order of 5Ni/SBA-15 (10.8%) < 3Ni/SBA-15 (13.3%) < 10Ni/SBA-15 (21.7%). It is evident that 5wt% Ni loading have lower amount of carbon deposition compared to the 3 wt% and 10 wt% Ni loading. This result can be explained by the presence metal-support interaction which prevents the Ni particle being carried away from the SBA-15 surface, thus minimizing the growth of encapsulating graphite carbon.

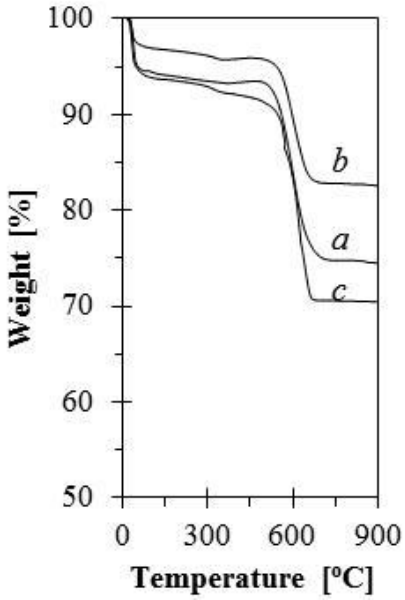

Figure 7: TGA curves of (a) spent 3Ni/SBA-15, (b) spent 5Ni/SBA-15 and (c) spent 10Ni/SBA-15 after 5 h reaction.

Conclusion

The influences of Ni loading (3 – 10 wt%) on the properties of Ni/SBA-15 and CO_2 reforming of CH_4 were studied, owing to the fact that metal loading has a significant influence on the metal-support interaction and catalytic performance of the catalyst. Characterization results indicated that the formation of Ni–O–Si by substitution of surface silanol groups with Ni species and the maximum substitution was achieved at 5 wt% loading, while further increase in Ni loading stimulate the agglomeration of Ni particles. The catalytic activity of Ni/SBA-15 towards CO_2 reforming of CH_4 followed the order of 5Ni/SBA-15 > 3Ni/SBA-15 ≈ 10Ni/SBA-15, whereas the average H_2/CO ratio followed the order of 5Ni/SBA-15 > 3Ni/SBA-15 > 10Ni/SBA-15. The superior catalytic behavior of 5Ni/SBA-15 towards CO_2 reforming of CH_4 probably was related to the presence of Ni–O–Si, which enhanced the stabilization of the active Ni species on SBA-15 and altered the properties of catalyst towards an excellent catalytic performance. In addition, the analysis of spent Ni/SBA-15 catalysts found that the presence of Ni–O–Si minimizes the growth of encapsulating graphite carbon and thus enhanced the stability of catalyst. Thus, the present study confirmed that metal-support interaction, Si–O–Ni played an important role in the enhancement of the catalytic performance of Ni/SBA-15 catalysts.

Acknowledgments -The authors are grateful for the financial support from Ministry of Education Malaysia through Fundamental Research Grant Scheme (RDU150126) and Universiti Malaysia Pahang through Research University Grant (RDU140391 & RDU140398).

References

1. Abderrahim H., Berrebia M., Hamou A., Kherief H., Zanoun Y., Zenata K., *J. Mater. Environ. Sci.* 2 (2) (2011) 94-103.
2. Sidik S.M., Triwahyono S., Jalil A.A., Aziz M.A.A., Fatah N.A.A., Teh L.P., *J. CO_2 Util.* 13 (2016) 71–80.
3. Ababou A., Ajbary M., Taleb M., Kherbeche A., *J. Mater. Environ. Sci.* 6 (9) (2015) 2367-2372.
4. Liu J., Cui D.M., Yu J., Su F.B., Xu G.W., *Chin. J. Chem. Eng.* 23 (1) (2015) 86–92.
5. Zhang J.Y., Xin Z., Meng X., Tao M., *Chin. J. Chem. Eng.* 65 (2014) 165–168 (in Chinese).
6. Donphai W., Faungnawakij K., Chareonpanich M., Limtrakul J., *Appl. Catal. A: Gen.* 475 (2014) 16–26.

7. Sajjadi S.M., Haghighi M., Eslami A.A., Rahmani F., *J. Sol-Gel Sci. Tech.* 67 (2013) 601–617
8. Theofanidis S.A., Galvita V.V., Poelman H., Marin G.B., *ACS Catal.* 5 (2015) 3028–3039.
9. Xu J., Lin Q., Su X., Duan H., Geng H., Huang Y., *Chin. J. Chem. Eng.* 24 (2016) 140–145.
10. Tao K., Zhang Y., Terao S., Tsubaki N., *Catal. Today* 153 (2010) 150–155.
11. Richardson J.T., Garrait M., Hung J.-K., *Appl. Catal. A: Gen.* 255 (2003) 69–82.
12. Nematollahi B., Rezaei M., Khajenoori M., *Int. J. Hydrogen Energy* 36 (2011) 2969–2978.
13. Khajenoori M., Rezaei M., Meshkani F., *J. Ind. Eng. Chem.* 21 (2015) 717–722.
14. Qi Y., Cheng Z., Zhou Z., *Chin. J. Chem. Eng.* 23 (2015) 76–85.
15. Liu Q., Dong X., Liu Z., *Chin. J. Chem. Eng.* 22(2) (2014) 131-135.
16. Liu D., Quek X.-Y., Wah H.H.A., Zeng G., Li Y., Yang Y., *Catal. Today* 148 (2009) 243–250.
17. Wang N., Yu X., Wang Y., Chu W., Lu M., *Catal. Today* 212 (2013) 98–107.
18. Wang S., Lu G.Q., *Appl. Catal. A: Gen.* 169 (1998) 271–280.
19. Martínez A., López C., Márquez F., Díaz I., *J. Catal.* 220 (2003) 486–499.
20. Setiabudi H.D., Jalil A.A., Triwahyono S., *J. Catal.* 294 (2012) 128–135.
21. Donphai W., Faungnawakij K., Chareonpanich M., Limtrakul J., *Appl. Catal. A: Gen.* 475 (2014) 16–26.
22. Kaydouh M.N., El Hassan N., Davidson A., Casale S., El Zakhem H., Massiani P., *Microporous Mesoporous Mater.* 220 (2016) 99–109.
23. Zhao D., Feng J., Huo Q., Melosh N., Fredrickson G.H., Chmelka B.F., Stucky G.D., *Science* 279 (1998) 548–552.
24. Hartmann M., Vinu A., *Langmuir* 18 (2002) 8010–8016.
25. Zhang M., Ji S., Hu L., Yin F., Li C., Liu H., *Chin. J. Catal.* 27 (2006) 777–781.
26. Lu B., Kawamoto K., *Fuel* 103 (2013) 699–704.
27. Cullity B.D., *Elements of X-ray Diffraction*, Second Edition, Addison-Wesley, Reading, MA, 1978.
28. Aziz M.A.A., Jalil A.A., Triwahyono S., Saad M.W.A., *Chem. Eng. J.* 260 (2015) 757–764.
29. Chanadee T., Chaiyarat S., *J. Mater. Environ. Sci.* 7 (7) (2016) 2369-2374
30. Brodie-Linder N., Le Caër S., Alam M.S., Renault J.P., Alba-Simionesco C., *Phys. Chem. Chem. Phys.* 12 (2010) 14188 –14195.
31. Setiabudi H.D., Triwahyono S., Jalil A.A., Kamarudin N.H.N., Aziz M.A.A., *J. Nat. Gas Chem.* 20 (2011) 477–482.
32. Oemar U., Kathiraser Y., Mo L., Ho X.K., Kawi S., *Catal. Sci. Technol.*, 6 (2016) 1173-1186.
33. Rahemi N., Haghighi M., Babaluo A.K., Allahyari S., Jafari M.F., *Energy Convers. Manag.* 84 (2014) 50-59.
34. Vafaeian Y., Haghighi M., Aghamohammadi S., *Energy Convers. Manag.* 76 (2013) 1093–1103.
35. Bradford M.C.J., Vannice M.A., *Catal. Lett.* 48 (1997) 31–38.
36. Son I.H., Lee S.J., Song I.Y., Jeon W.S., Jung I., Yun D.J., Jeong D.-W., Shim J.-O., Jang W.-J., Roh H.-S., *Fuel* 136 (2014) 194–200.